



ISSN: 2230-9926

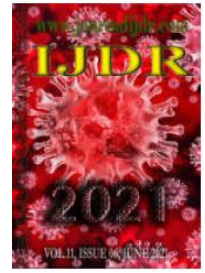
Available online at <http://www.journalijdr.com>

IJDR

International Journal of Development Research

Vol. 11, Issue, 06, pp. 48141-48147, June, 2021

<https://doi.org/10.37118/ijdr.22207.06.2021>



RESEARCH ARTICLE

OPEN ACCESS

MAGNETIC AND MICROSTRUCTURAL PROPERTIES MEASUREMENT AND ANALYSIS OF THE SMCs MATERIALS COATED BY DOUBLE INSULATING LAYER

Jaime Andre Back^{1,*}, Jeferson Camilotti Gaio², Lírio Schaeffer², Andrison Rodrigues Teixeira³

¹Electrical Engineer, Federal University of Rio Grande do Sul (PPGE3M/UFRGS), Porto Alegre, Brazil

²Mechanical Engineer, Federal University of Rio Grande do Sul (PPGE3M/UFRGS), Porto Alegre, Brazil

ARTICLE INFO

Article History:

Received 27th June, 2021

Received in revised form
29th June 2021

Accepted 08th July, 2021

Published online 10th July, 2021

Key Words:

Soft Magnetic Composite,
Coated Iron Powder,
Insulating Thin-Layers,
Phosphate, Oxide, Resin.

*Corresponding author:

Jaime Andre Back

ABSTRACT

This work presents the study of the preparation routes of a soft magnetic composite (SMC) with an insulating iron-phosphate-resin coating. The energy losses of these composite materials in relation to the mobility of the domain walls during the magnetization process were studied. The SMC concept is based on the coating of magnetic particles with a surface layer, in the order of nanometers, electrically insulating and joined in the form of a three-dimensional matrix of a finished compact. The amount of phosphoric acid dissolved in the solvent should correspond to the desired coating thickness on the coated powder particles, where it was found that a suitable concentration of H_3PO_4 in 1 liter of acetone was 1/20 parts, to be added later 30 ml to 100 ml for 1000 grams of iron powder. The magnetic properties were investigated from the DC and AC hysteresis curve in the 0.05 Hz to 260 Hz frequency range and measured in relation to the contribution of the magnetic flux of the non-ferromagnetic components (pores and resin). The total losses were calculated from the area of the hysteresis loops, where the maximum values of 300, 420 and 600 W/m^3 were found. The values of the maximum magnetic flux density B_m were around (0.82, 0.78 and 0.62 T), for frequencies of 1, 50 and 260 Hz, respectively.

Copyright © 2021, Jaime Andre Back et al. This is an open access article distributed under the Creative Commons Attribution License, which permits unrestricted use, distribution, and reproduction in any medium, provided the original work is properly cited.

Citation: Jaime Andre Back, Jeferson Camilotti Gaio, Lírio Schaeffer and Andrison Rodrigues Teixeira. "Magnetic and microstructural properties measurement and analysis of the smcs materials coated by double insulating layer", *International Journal of Development Research*, 10, (11), 48141-48147.

INTRODUCTION

Soft Magnetic Composites (SMCs) are a recent advancement of the well-known and well-established Soft Magnetic Materials (SMMs). Possessing specific soft magnetic properties such as high saturation magnetization, stable permeability and low core loss at intermediate frequencies, having a wide range of applications when used in energy conversion (Zhou, 2020; Sunday, 2017; Hu, 2020). The SMC concept is based on the coating of magnetic particles with a surface layer, in the order of nanometers, electrically insulating and joined in a three-dimensional matrix form of a finished compact. During its use as a magnetic material, it must be magnetized along the different directions of the grains, so that, ideally, it should have the same behavior in each of these, that is, the absence of magno-crystalline anisotropy (Gavrila, 2002; Hanejko, 1996).

Thus, uniform 3D magnetic properties are acquired due to the isotropic nature of this material, which provides greater freedom in creating more complex designs (design flexibility) (Lei, 2019; Birčáková, 2020). Because it is integrated into an electrical machine design, the SMC material can improve the magnetic performance of these motors, in addition to reducing parts and facilitating the integration between parts, as the magnetic cores are molded into a single piece by compacting particles by tape. Magnetic strips coated with an insulating layer to prevent the formation of eddy currents (Guo, 2008; Jack, 2003). This insulation is directly related to the type of coating, uniform coating layer, particle coating structure and suitable preparation process (Hu, 2020; Sunday et al., 2017). As for the particles, they can be made of different types of materials, such as pure iron (99.98%). Different types of coatings can be applied on the magnetic particles to form the insulating layer, being divided into organic and inorganic, metallic and non-metallic layers. Insulating layers treated with phosphoric acid (H_3PO_4) are described in papers

(Xia, 2019; Chen, 2019; Chen, 2020) and in patents (Jansson, 2002; Maeda, 2010; Ye, 2012; Ye, 2018), together with the addition of some type of oxide in the solution. An insulator of oxide can be used, such as, in addition to iron phosphate, manganese phosphate, zinc phosphate, calcium phosphate, aluminum phosphate, silicon oxide, titanium oxide, aluminum oxide or zirconium oxide. In addition to the layers formed with phosphate and oxides, other types of compositions and coating methods are studied, in order to ensure a thinner and more homogeneous layer, improving the electrical isolation between the particles, their magnetic and mechanical responses. Some examples include the addition of zinc the use of boron oxide (Ishizaki, 2017; Evangelista, 2020), and glassy layers containing silica and silicates (Tontini, 2017; Hu *et al.*, 2020).

Literature Review

Soft Magnetic Materials (SMMs) can be easily magnetized and demagnetized. The most important characteristics desired for a soft magnetic material are high magnetic saturation B_s , high permeability, low coercivity H_c and low core losses. The correlation between magnetic flux density B and magnetic field strength H is described by the hysteresis curve or B - H curve, as shown in Figure 1.

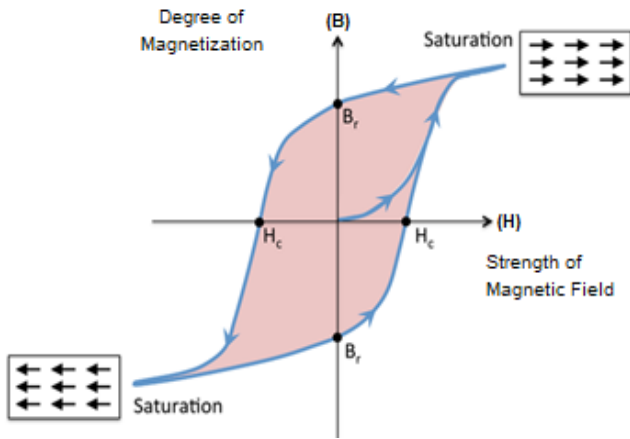


Figure 1. Hysteresis cycle for a demagnetized ferromagnetic material (27)

Furthermore, the magnetic properties of these materials depend on their chemical composition and microstructure. For example, the saturation induction rate mainly depends on the chemical composition. Coercivity, remanence and permeability depend on the microstructure of the magnetic material. As cold deformation, heat treatment, grain size and impurities strongly influence the microstructure, magnetic properties are similarly influenced (Lefebvre *et al.*, 1997).

Soft Magnetic Composites: An SMC can be understood as a mass multiphase system where at least one dielectric phase coats an SMM originally in powder form, and which is normally produced using Powder Metallurgy techniques in the compaction and heat treatment/curing/annealing procedures (Sunday, 2017). The magnetic response of an SMC as a function of the magnitude and frequency of the applied external field is a topic of frequent investigation due to its importance in electromagnetic applications and depends on several characteristics of each of the phases (including chemical composition, volume fraction and distribution and the presence of defects) (Giménez *et al.*, 2006). Therefore, in order to understand and develop improved SMCs, as well as to characterize them adequately, a multidisciplinary approach involving scientific and technical aspects is necessary (Pérido *et al.*, 2018). SMCs, like any other engineering SMM, are expected to exhibit minimal energy loss in combination with low k magnetostriction (variation in physical dimension when a magnetic field is present in the environment), high saturation polarization B_s (related to the orientation of magnetic moments per unit volume of the magnetic material), and the greatest possible permeability.

Soft magnetic compounds mainly consist of ferromagnetic particles that are coated with an insulating layer (Shokrollahi, 2017). There are different variations of particles and insulators that are powder metallurgically processed into a complex composite material. Pure Fe powder, iron alloys with e. Ni, Co, Si as well as amorphous and nanocrystalline materials are the common materials for powder particles (Nowosielski, 2007). Particle coatings are generally divided into two categories: organic and inorganic coatings. Inorganic coatings are, for example, zinc, iron or manganese phosphates, metal oxides and sulphates. Organic coatings are divided into thermoplastic or thermosetting resin coatings. There are also inorganic-organic hybrid coatings (Slovaca *et al.*, 2013; Gramatyka, 2006).

Magnetic Properties: The properties of soft magnetic composites include magnetic and thermal isotropy, very low eddy current loss, and relatively low total core loss at frequencies in the mid-range frequency. It also has high magnetic permeability, high remanent magnetization, high resistivity and low coercivity (Asaka, 2005). The magnetic permeability of SMC is directly influenced by the type of insulating material, which can be organic or inorganic. The insulating coating on powder particles of SMCs eliminates the current paths from particle to particle (Figure2), thus minimizing eddy current losses. However, this coating also reduces permeability due to the creation of non-magnetic spaces between the particles (*gap*) and, to some extent (proportional to the volume fraction of the coating), the saturation magnetization of the compound. To provide maximum magnetic permeability, therefore, the amount of insulation must be minimized and the ferromagnetic content must be maximized (Sato *et al.*, 2015).

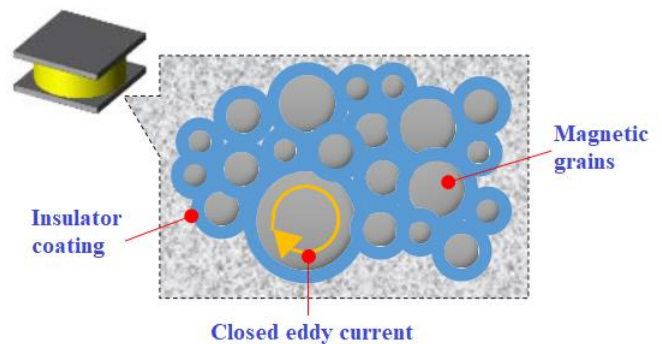


Figure 2. Insulating coating on an SMC concentrated on a coated particle [36]

In addition to the coating thickness, the maximum magnetic permeability of the SMC is also limited by the presence of air gaps (pores) in the direction of magnetic flux circulation due to the cavities of the iron particles. This material porosity is directly related to the compaction pressure level (Cyr, 2009). The designer of a new SMC material always tries to increase magnetic permeability while keeping electrical resistivity and mechanical strength sufficiently balanced.

Magnetic Losses in SMCs: The general picture of energy losses is based on the Joule effect of eddy currents induced by changes in magnetic flux density following the domain wall displacement and magnetization vector rotation, both in the process of direct and alternating current magnetization (Coey, 2009; Buschow, 2005). Losses in soft magnetic materials can be divided into hysteresis cycle losses (W_H), eddy current losses (W_{CL}), and anomalous or excess losses (W_{EXC}). Eddy current losses within an iron core occur due to the decrease in electrical resistance that the alternating electric field creates. Two main effects are observed in materials when eddy currents are induced: incomplete magnetization of the material and increase in core losses.

Unlike eddy current losses (more prominent with increasing frequency), hysteresis losses are the main factor at low frequencies and can be reduced using high purity iron, larger particle size and annealing step for stress relief of compression (Pérido *et al.*, 2018). Generally, in addition to the electrical resistivity of the ferromagnetic

material, classical losses are also defined by the geometry of the sample, especially the effective dimension that determines the flow of eddy currents in the cross-section of the sample. Also in SMCs eddy currents can flow in the cross section of an entire sample in the case of non-perfect isolated particles (inter-particle eddy currents), as illustrated in Figure 3. Furthermore, in SMCs it is necessary to consider that the eddy currents are closed inside the ferromagnetic particles (intra-particle eddy currents) (Pérido *et al.*, 2018).

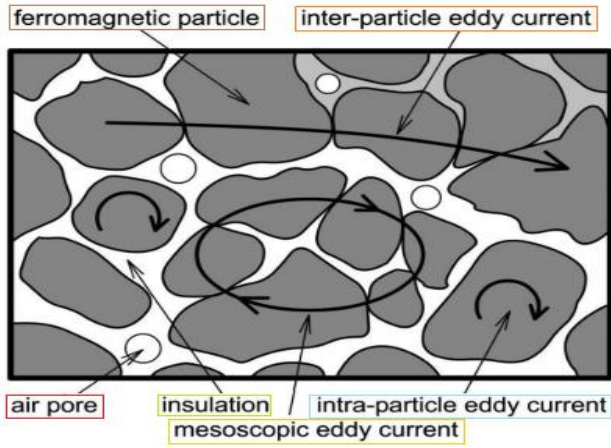


Figure 3. Schematic of the paths taken by eddy currents in an SMC [30]

Particle Coating on SMCs: The insulating coating that individually separates the iron powder particles in an SMC product is the key feature of this technology. Its thickness, coverage and resistance under different processing operations are fundamental aspects for the properties of a magnetic part. In this context, different strategies to obtain a suitable coating for magnetic applications are the subject of numerous studies. Yang *et al.* (Yang, 2017) present the results of the development of a nanostructured FeCo/CoFe₂O₄ composite produced by the controlled oxidation of FeCo particles. High purity 60 nm thick CoFe₂O₄ layers can be formed in-situ on the surface of unoxidized FeCo particles to form a high density core-shell structure. The best intrinsic magnetic properties, including a high saturation magnetization and a low coercivity, are obtained in these composites due to the nano-thickness of the ferrimagnetic layers. A CoFe₂O₄ shells can be formed in-situ on the surface of the micron-sized FeCo particles by controlled oxidation according to Figure 4.

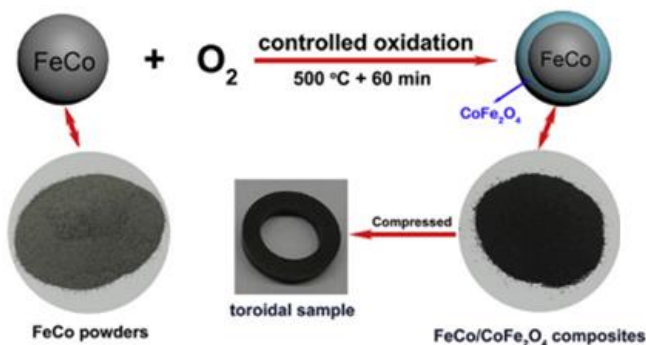


Figure 4. Schematic illustration and the technical process of controlled oxidation for FeCo/CoFe₂O₄ composites [35]

In the work by Meng *et al.* (2019), a coating strategy for producing high performance metal-based magnetic compounds exhibiting high magnetic inductions and lower core loss is presented. High purity FeCo particles were dispersed in silicone resin to form a magnetic insulating film, which was then uniformly coated on the surface of the Fe powder particle with a particle size of 170 μm to form a new type SMC. These insulated magnetic layers can maintain a very high saturated magnetization for composites and also result in

their low core loss. The schematic illustration for the preparation of these new types of Fe and resin based SMCs is shown in Figure 5.

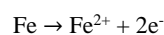
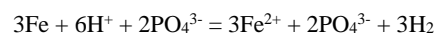


Figure 5. A schematic illustration for the preparation of Fe-based SMCs coated with magnetic insulating layers [36]

The frequency dependence of the energy losses of iron-phenol-formaldehyde resin composite materials on the mobility of domain walls during the magnetization process is studied in Birčáková *et al.* (Huang *et al.*, 2015). The usual concept of three-component separation of total losses is proposed for the case of magnetic composites, introducing simplifications in the calculation of classical losses and pointing out the different frequency dependence of excess (anomalous) losses compared to homogeneous materials, which is explained by the different frequency dependencies of a series of moving domain walls. Experimental results in samples with different resin contents confirmed the explanation and revealed the influence of internal demagnetizing fields on the activation of the domain walls. Finally, Huang *et al.* (Kopeliovich, 2013) describes the preparation of phosphate layers as an insulating coating for Fe and FeSiAl soft magnetic composites and the mechanisms of the phosphatization process were investigated. For Fe SMCs as a powder base, the insulating coating mainly consists of iron phosphate after surface passivation. For FeSiAl SMCs, the phosphate coating mainly contains Al(PO₃), which converts to oxides like Al after annealing. These oxides have high electrical resistivity and continue to serve as an insulating coating for composites.

The Phosphating Process: Phosphating is a well-known metal conversion treatment, especially in the automotive industry. It is used to provide the material with a thin layer of a phosphate coating that imparts anti-corrosion and wear-resistant properties to the surface. Thus, the steps of the phosphating process are as follows: (i) Surface cleaning (blasting); (ii) Rinse material in hot water; (iii) phosphating by immersion of the material in a phosphate bath or by spraying; (iv) rinsing with water; and (v) drying. The main components of a conventional phosphating solution are: (i) phosphoric acid (H₃PO₄); (ii) water or acetone as the main solvent; (iii) ions (typically cations) of divalent metals such as Zn²⁺, Fe²⁺, Mn²⁺; and (iv) accelerator – if you want to increase the rate of the coating process and reduce the grain size of the deposited coating. It is usually an oxidizing reagent such as nitrate, nitrite or peroxide.

When a metallic material, for example iron, is immersed in a phosphate solution, iron ions are supplied by the dissolving substrate and a chemical top-up reaction takes place at the surface. There, the iron dissolution is initiated in the micro-anodes present in the substrate by the free phosphoric acid present in the bath (43). Hydrogen evolution occurs at micro-cathode sites according to the following equations:



A simplified schematic of the phosphating process is shown in Figure 6. As these reactions proceed, the pH is locally lowered at the surface. Then, the metal surface becomes first covered by a thin layer of primary ferrous phosphate which is water soluble and then a thicker insoluble tertiary and secondary ferrous phosphate given by the reactions below:

- Primary ferrous phosphate (soluble):

$$\text{Fe} + 2\text{H}_3\text{PO}_4 = \text{Fe}(\text{H}_2\text{PO}_4)_2 + \text{H}_2$$
- Secondary ferrous phosphate (insoluble):

$$\text{Fe} + \text{Fe}(\text{H}_2\text{PO}_4)_2 = 2\text{FeHPO}_4 + \text{H}_2$$
- Tertiary ferrous phosphate (insoluble):

$$3\text{Fe}^{2+} + 2\text{PO}_4^{3-} = \text{Fe}_3(\text{PO}_4)_2$$

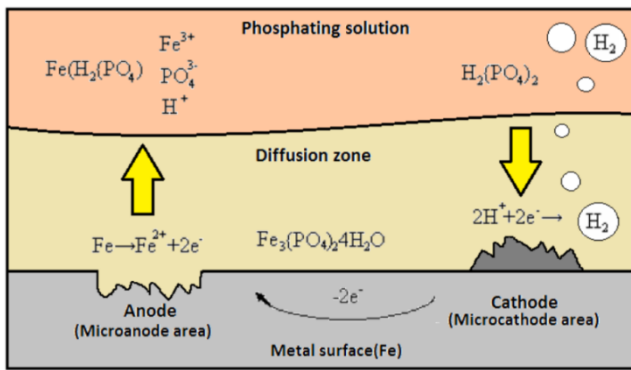


Figure 6. Scheme of the iron surface phosphating process [43]

The existing ions are hydrogen anions and the resulting coating is iron phosphate, as indicated by chemical reactions. The treatment is carried out by stirring the iron powder continuously in the solution bath to expose each particle. During the process, a small amount of metal is removed from the surface and then deposited irregularly. However, this etching also has the side effect of permanently removing some of the metal, as not all of it is deposited again.

MATERIALS AND METHODS

The characterization of SMCs materials can be done by means of specimens, which provided the analysis of the physical and magnetic properties of each material, comparing these with existing results in the literature.

The Phosphating Process: When using the phosphating method to provide insulating coatings, a layer thickness more suitable for electromagnetic applications should be sought. For example, using phosphoric acid concentrations that provide improved electrical insulation properties, but resistivity can be increased to some extent. The amount of phosphoric acid dissolved in the solvent should correspond to the desired coating thickness on the coated powder particles as defined below. A suitable concentration of phosphoric acid in acetone has been found to be between 30 ml to 100 ml of phosphoric acid per liter of acetone. The appropriate amount of solution (acetone + phosphoric acid) to be added is 50 to 150 ml for 1000 grams of iron powder.

Consequently, one can only use phosphoric acid in a solvent at such concentrations and treatment times in order to obtain the relationship between particle size, layer thickness and its homogeneity. Then the powder is dried at 80 °C for 30 minutes. Figure 7 shows the samples of Fe phosphatized with different phosphate solutions, being (a) Granulated iron due to very thick phosphating, without dilution in acetone and (b) Phosphate diluted in acetone (1 part phosphoric acid to 10 parts acetone) where it does not have excessive grain.

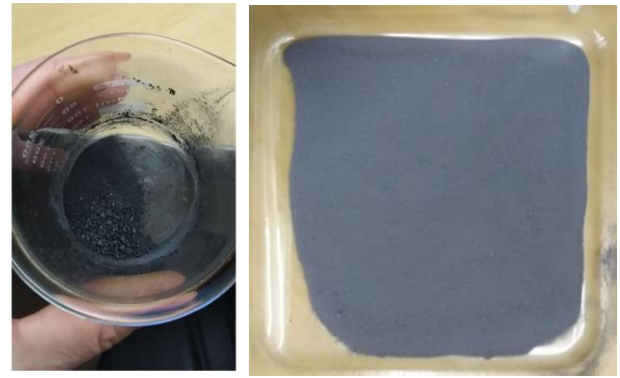


Figure 7. Granulated iron due to very thick phosphatization, without dilution in acetone and Phosphate diluted in acetone.

Design Parameters for Magnetic Tests: For the hysteresis test, it is necessary to prepare a ferromagnetic sample, which can, for example, be in a ring format, as shown in Figure 8. This ring must then be wound (winding of the primary and secondary coils and in the ring), with each beret containing n turns, starting with the secondary winding, in order to be closer to the material.

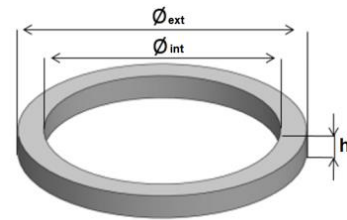


Figure 8. Preparation of a ring-shaped ferromagnetic sample

These tests are used to measure the rate of energy loss and produce characteristic graphs of the hysteresis and magnetization cycle in electrical materials. However, to do so, the following equations must be taken:

Calculate the Cross Section S_T , in mm^2 :

$$S_T = \left(\frac{\phi_{ext}}{2} - \frac{\phi_{int}}{2} \right) \times h$$

Calculate the density of the sintered ring using the equation below:

$$d = \frac{massa}{\pi \cdot h \cdot \left(\frac{\phi_{ext}^2}{4} - \frac{\phi_{int}^2}{4} \right)}$$

Calculate the primary expiratory density by Equation, given the importance of this parameter for calculating the hysteresis curve of the material:

$$d_{pri} = \frac{N_p}{\pi \left(\frac{\phi_{ext} + \phi_{int}}{2} \right)}$$

Where ϕ_{ext} is the outside diameter, ϕ_{int} is the inside diameter, h is the height, d is the ring density, d_{pri} being the primary expiration density (turns/mm) and N_p number of primary turns.

Computational Measurement Methodology: In its simplest realization, the continuous recording method employs a magnetizing current source, realized with a function generator and a power amplifier, and a flux measurement device connected to the secondary winding, and subsequent data discretization by using analog-to-digital (A/D) conversion (Fiorillo, 2010). Considering the diagram in Figure 9-a, the amplitude and waveform are usually adjusted by the signal generator (1). Its output signal drives the power amplifier (2).

The primary winding with turns N_i is connected to the output of the power amplifier, in series with a precision, low-inductance shunt resistor R . The voltage drop $U_1 = R \cdot I$ across the shunt is proportional to the strength of the magnetic field H at sample. The voltage U_2 that is

induced in the secondary winding is proportional to the flux variation $d\Phi/dt$. Flux density B is obtained from U_2 by numerical integration. Both voltages U_1 and U_2 are sampled synchronously by two fast A/D converters (4). The resulting data is stored on the PC and the hysteresis cycle is displayed (Figure 9-b).

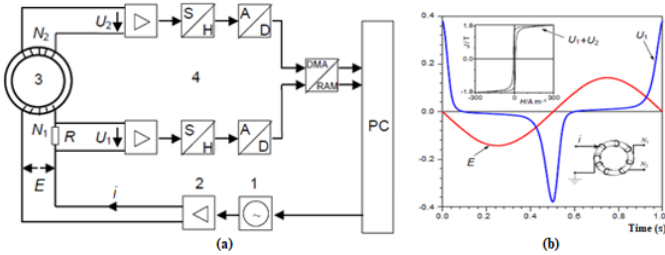


Figure 9. Diagram of the measurement principle (a) and Example of final voltage signals in the primary circuit over a period and the hysteresis loop, shown in the insert (b), at 1 Hz [38]

RESULTS AND DISCUSSION

A sample was prepared by the phosphatization method, using the technique of immersing iron powder in a liquid solution of acetone + phosphoric acid. The iron base powder was immersed in a concentration of 1/20 parts of phosphoric acid for 5 minutes and then dried at 85 °C for 45 minutes. The characterization of these materials can be done by means of specimens, which provided the analysis of the physical and magnetic properties of each material, comparing them with existing results in the literature. Figure 10 shows the compacted samples in the form of a ring (a); the sample already coiled after heat treatment (b); and a sample removed from the ring for analysis by SEM micrograph (c).

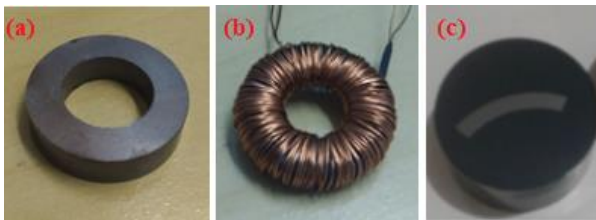


Figure 10. Samples in the form of a ring of powder coated with Fe_2O_3 , H_3PO_4 and resin: (a) Compacted samples in the form of a ring; (b) The sample already coiled after heat treatment; (c) Sample removed from the ring for analysis by SEM micrograph

Figure 11 shows the fracture area of the ring specimens observed by light microscopy showing iron particles coated by oxide, phosphate and by the addition of resin. The density of the SMC was 7.14 g/cm^3 , while the porosity was calculated from the mass and dimensions of the samples (densities - iron: 7.85 g/cm^3 , resin: 1.37 g/cm^3).

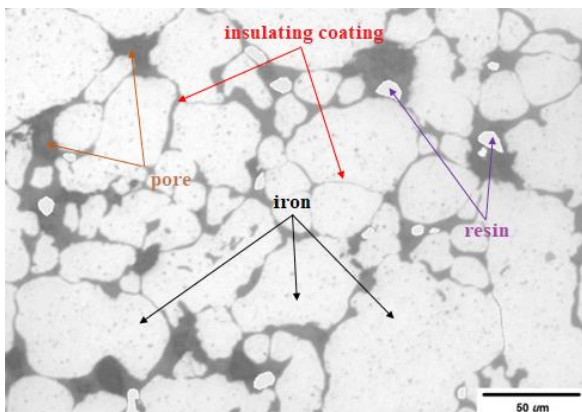


Figure 11. Scanning electron microscopy (SEM) observation of a sample after heat treatment of the sample

In samples with higher phosphate content, the insulating layers become too thick, which causes an increase in electrical resistivity, thus decreasing the magnetic permeability of the SMC. The higher resin content, on the other hand, causes a greater dynamics in W_D or losses and the total energy losses W_T increased with increasing frequency and more abruptly (despite the lower classical interparticle losses due to the higher specific resistivity of samples with higher content of resin). This can be caused by higher classical $W_{intraparticle}$ losses due to particle aggregation (larger mean particle diameter) or by higher excess W_{EXC} losses due to fewer moving domain walls.

Magnetic properties were investigated from the DC and AC hysteresis curve (Figure 12) and measured in relation to the magnetic flux contribution of the non-ferromagnetic components (pores and resin) that were subtracted.

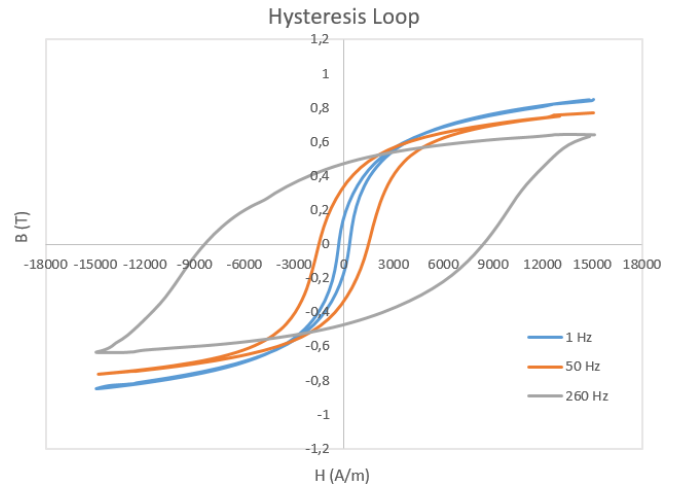


Figure 12. Hysteresis loop test of samples in powder coated ring form. The values of the maximum magnetic flux density B_m around (0.82, 0.78 and 0.62 T).

AC and DC hysteresis curves were measured in the frequency range 1 Hz, 50 Hz and 260 Hz. The total losses were calculated from the area of the hysteresis loops, where the maximum values of 300, 420 and 600 W/m^3 were found (Figure 13). It can be seen that the increase in losses is proportional to the increase in frequency. This is justified mainly due to the thickness of the insulating layer.

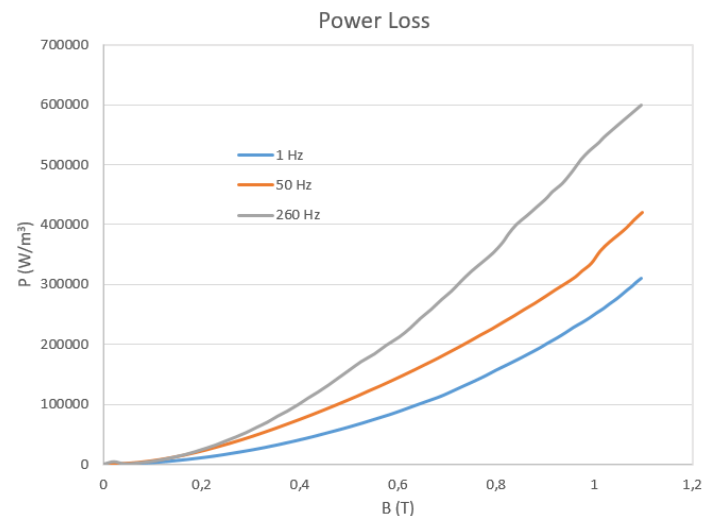


Figure 13. Total losses calculated under the area of the hysteresis loops, with maximum values of 300, 420 and 600 W/m^3 for 1, 50 and 260 Hz, respectively

CONCLUSION

The aim of this study was the development of a soft magnetic composite SMC from the coating of iron particles with the superposition of a phosphate layer (H_3PO_4) on an oxide (Fe_2O_3). The resin insertion determines the magnitude of the interaction between particles, as well as the dependence of the mobility of the domain walls on the insulation content.

The lower the resin content, the smaller the internal demagnetization fields and the stronger the magnetic interaction between the particles, resulting in a greater number of moving domain walls needed for magnetic reversal. In samples with higher H_3PO_4 content, the insulating layers become very thick, which causes an increase in electrical resistivity, thus decreasing the magnetic permeability of the SMC. The total losses were calculated from the area of the hysteresis loops, where the maximum values of 300, 420 and 600 W/m^3 were found. The values of the maximum magnetic flux density B_m were around (0.82, 0.78 and 0.62 T), for frequencies of 1, 50 and 260 Hz, respectively. However, the total losses increased with increasing frequency, mainly due to the excess of pores found in the samples studied in this work.

Acknowledgment

The authors wish to thank the Federal University of Rio Grande do Sul (UFRGS), in particular to the Graduate Program in Mining, Metallurgy and Materials Engineering (PPGE3M) and to the Technology and Mechanical Transformation Center (LdTM).

REFERENCES

- Zhou, B. *et al.* 2020. 'Fe-based amorphous soft magnetic composites with SiO₂ insulation coatings: A study on coatings thickness, microstructure and magnetic properties', *Ceramics International*, 469, pp. 13449–13459. doi: 10.1016/j.ceramint.2020.02.128.
- Sunday, K. J. and Taheri, M. L. 2017. 'Soft magnetic composites: recent advancements in the technology', *Metal Powder Report*, 726, pp. 425–429. doi: 10.1016/j.mprp.2016.08.003.
- Hu, W. *et al.* 2020. 'Prepared novel Fe soft magnetic composites coated with ZnO by ZnCH₃COO₂ pyrolysis', *Journal of Magnetism and Magnetic Materials*, 505, p. 166744. doi: 10.1016/j.jmmm.2020.166744.
- Gavrila, H. and Ionita, V. 2002. 'Crystalline and amorphous soft magnetic materials and their applications - Status of art and challenges', *Journal of Optoelectronics and Advanced Materials*, 42, pp. 173–192.
- Hanejko, F. G. *et al.* 1996. 'Powder Metallurgy Materials for AC Magnetic Applications'.
- Lei, J. *et al.* 2019. 'Effects of heat treatment and lubricant on magnetic properties of iron-based soft magnetic composites with Al₂O₃ insulating layer by one-pot synthesis method', *Journal of Magnetism and Magnetic Materials*, 472 July 2018, pp. 7–13. doi: 10.1016/j.jmmm.2018.09.125.
- Luo, Z. *et al.* 2019. 'Controllable SiO₂ insulating layer and magnetic properties for intergranular insulating Fe-6.5wt. Si/SiO₂ composites', *Advanced Powder Technology*, 303, pp. 538–543. doi: 10.1016/j.apt.2018.12.004.
- Nikas, D. 2013. *Characterization of electrically insulating coatings for soft magnetic composite materials by means of surface sensitive analytical techniques*. Chalmers University of Tech.
- Xia, C. *et al.* 2019. 'The magnetic properties and microstructure of phosphated amorphous FeSiCr/silane soft magnetic composite', *Journal of Magnetism and Magnetic Materials*, 474, pp. 424–433. doi: 10.1016/j.jmmm.2018.11.058.
- Kollár, P. *et al.* 2013. 'Power loss separation in Fe-based composite materials', *Journal of Magnetism and Magnetic Materials*, 327, pp. 146–150. doi: 10.1016/j.jmmm.2012.09.055.
- Zhou, B. *et al.* 2019. 'The core-shell structured Fe-based amorphous magnetic powder cores with excellent magnetic properties', *Advanced Powder Technology*, 308, pp. 1504–1512. doi: 10.1016/j.apt.2019.04.027.
- Birčáková, Z. *et al.* 2020. 'Preparation and characterization of iron-based soft magnetic composites with resin bonded nano-ferrite insulation', *Journal of Alloys and Compounds*, 828, p. 154416. doi: 10.1016/j.jallcom.2020.154416.
- Guo, Y. *et al.* 2008. 'Influence of inductance variation on performance of a permanent magnet claw pole soft magnetic composite motor', in *Journal of Applied Physics*. doi: 10.1063/1.2834397.
- Jack, L. O. and Hultman, A. G. 2003. 'Soft Magnetic Composites - Materials and Applications', pp. 516–522.
- Sunday, K. J., Hanejkob, F. G. and Taheria, M. L. 2017. 'Magnetic and microstructural properties of Fe₃O₄-coated Fe powder soft magnetic composites', *Journal of Magnetism and Magnetic Materials*, 423, pp. 164–170. doi: 10.1016/j.jmmm.2016.09.024.
- Chen, Z. *et al.* 2019. 'Phosphate coatings evolution study and effects of ultrasonic on soft magnetic properties of FeSiAl by aqueous phosphoric acid solution passivation', *Journal of Alloys and Compounds*, 783, pp. 434–440. doi: 10.1016/j.jallcom.2018.12.328.
- Chen, Y. *et al.* 2020. 'Enhanced magnetic properties of iron-based soft magnetic composites with phosphate-polyimide insulating layer', *Journal of Alloys and Compounds*, 813, p. 152205. doi: 10.1016/j.jallcom.2019.152205.
- Ishizaki, T. *et al.* 2017. 'Improving powder magnetic core properties via application of thin, insulating silica-nanosheet layers on iron powder particles', *Nanomaterials*, 71, . doi: 10.3390/nano7010001.
- Jansson, P. and Larsson, L.-A. 2002. 'Phosphate Coated Iron Powder And Method For The Manufacturing Thereof', *United States Patent*.
- Maeda, T. *et al.* 2010. 'Method of producing soft magnetic material soft magnetic powder, and dust core', *United States Patent*.
- Ye, Z. and Skarman, B. 2012. 'SOFT MAGNETIC POWDER', *United States Patent*.
- Ye, Z. and Staffansson, H. 2018. 'Nueva composición de polvo compuesto basado en hierro y método de fabricación para el componente de polvo', *OFICINA ESPAÑOLA DE PATENTES Y MARCAS*.
- Evangelista, L. L. *et al.* 2020. 'Developments on soft magnetic composites with double layer insulating coating: Synergy between ZnO and B₂O₃', *Journal of Magnetism and Magnetic Materials*, 497, p. 166023. doi: 10.1016/j.jmmm.2019.166023.
- Tontini, G. 2017. *Estudo de Compósitos Magnéticos Moles de Ferro Recoberto por Suspensão de Nanopartículas de Alumina em Vidro Líquido*. Universidade Federal de Santa Catarina - UFSC.
- Luo, Z. *et al.* 2020. 'High performance Fe-Si soft magnetic composites coated with novel insulating-magnetic-insulating IMI. layer', *Journal of Magnetism and Magnetic Materials*, 496 September 2019, p. 165937. doi: 10.1016/j.jmmm.2019.165937.
- Hu, F. *et al.* 2020. 'Low melting glass as adhesive and insulating agent for soft magnetic composites: Case in FeSi powder core', *Journal of Magnetism and Magnetic Materials*, 501, p. 166480. doi: 10.1016/j.jmmm.2020.166480.
- Coe, J. M. D. 2009. *Magnetism and Magnetic Materials*.
- Lefebvre, L. P., Pelletier, S. and Gélinas, C. 1997. 'Effect of electrical resistivity on core losses in soft magnetic iron powder materials', *Journal of Magnetism and Magnetic Materials*, 1762–3, pp. 93–96. doi: 10.1016/S0304-885397.01006-8.
- Giménez, S. *et al.* 2006. 'Effects of microstructural heterogeneity on the mechanical properties of pressed soft magnetic composite bodies', *Journal of Alloys and Compounds*, 4191–2, pp. 299–305. doi: 10.1016/j.jallcom.2005.09.053.
- Pérido, E. A. *et al.* 2018. 'Past, present, and future of soft magnetic composites', *Applied Physics Reviews*, 53, . doi: 10.1063/1.5027045.
- Shokrollahi, H. and Janghorban, K. 2007. 'Soft magnetic composite materials SMCs.', *Journal of Materials Processing Technology*. Elsevier, pp. 1–12. doi: 10.1016/j.jmatprotec.2007.02.034.

- Nowosielski, R. 2007. 'Soft magnetic polymer-metal composites consisting of nanostructural Fe-basic powders', *Journal of Achievements in Materials and Manufacturing Engineering*, 241. , pp. 68–77.
- Slovaca, A. M., Metall, A. and Conf, S. 2013. 'Improvement of mechanical properties of SMC through different hybrid inorganic-organic insulating coatings', 3, pp. 120–127. doi: 10.12776/amsc.v3.115.
- Gramatyka, P. *et al.* 2006. 'Soft magnetic composite based on', 151. , pp. 27–31.
- Asaka, K. and Ishihara, C. 2005. 'Technical trends in soft magnetic parts and materials', *Hitachi Powdered Metals Technical Repor*, 4, pp. 3–9.
- Sato, T. *et al.* 2015. 'Loss computation of soft magnetic composite inductors based on interpolated scalar magnetic property', *IEEE Transactions on Magnetics*, 513. , pp. 2–5. doi: 10.1109/TMAG.2014.2359983.
- Cyr, C. *et al.* 2009. 'Methodology to study the influence of the microscopic structure of soft magnetic composites on their global magnetization curve', *IEEE Transactions on Magnetics*, 453. , pp. 1178–1181. doi: 10.1109/TMAG.2009.2012544.
- Yang, B. *et al.* 2017. 'Oxidation fabrication and enhanced soft magnetic properties for core-shell FeCo/CoFe₂O₄ micron-nano composites', *Materials and Design*, 121, pp. 272–279. doi: 10.1016/j.matdes.2017.02.073.
- Buschow, K. H. J. 2005. *Concise encyclopedia of magnetic and superconducting materials*, *Bulletin of Materials Science*. doi: 10.1007/bf02745311.
- Meng, B. *et al.* 2019. 'Low-loss and high-induction Fe-based soft magnetic composites coated with magnetic insulating layers', *Journal of Magnetism and Magnetic Materials*, 492, p. 165651. doi: 10.1016/j.jmmm.2019.165651.
- Huang, M. *et al.* 2015. 'Evolution of phosphate coatings during high-temperature annealing and its influence on the Fe and FeSiAl soft magnetic composites', *Journal of Alloys and Compounds*, 644, pp. 124–130. doi: 10.1016/j.jallcom.2015.04.201.
- Kopeliovich, D. 2013. *Phosphate coating*, *Substances & Technologies*. Available at: http://www.substech.com/dokuwiki/doku.php?id=phosphate_coating.
- Fiorillo, F. 2010. 'Measurements of magnetic materials', *Metrologia*, 47, pp. 114–142.